CALIBRATION OF X-RAY MONITOR DURING THE PHASE I OF SuperKEKB COMMISSIONING

Emy Mulyani*, SOKENDAI, 1-1 Oho Tsukuba Ibaraki 305-0801, Japan
J.W Flanagan[1], KEK, 1-1 Oho Tsukuba Ibaraki 305-0801, Japan
[1] also at SOKENDAI, 1-1 Oho Tsukuba Ibaraki 305-0801, Japan

Abstract

X-ray monitors (XRM) have been installed in each SuperKEKB ring, the Low Energy Ring (LER) and High Energy Ring (HER), primarily for vertical beam size measurement. Both rings have been commissioned in Phase I of SuperKEKB operation (February-June 2016), and several XRM calibration studies have been carried out. The geometrical scale factors seems to be well understood for both LER and HER. The emittance knob ratio method yielded results consistent with expectations based on the machine model optics (vertical emittance ϵ_y is ≈8 pm) for the LER. For the HER, the vertical emittance ϵ_y is ≈41 pm, which is 4× greater than the optics model expectation. Analysis of beam size and lifetime measurements suggests unexpectedly large point response functions, particularly in the HER.

INTRODUCTION

The SuperKEKB accelerator is designed to collide e^-e^+ at a design luminosity of 8×10^{35} cm^{-2} s^{-1}(40× larger than that of KEKB)[1]. Measuring and controlling parameters of the accelerator beams is essential to achieve maximum performance from the accelerator; e.g., it is necessary to keep the single-beam vertical size small in order to obtain high luminosity. The XRMs have been installed in both SuperKEKB rings for vertical beam size measurement. Several XRM calibration studies have been carried out during the Phase I of SuperKEKB commissioning.

XRM APPARATUS

Two XRMs have been installed at SuperKEKB: one for electrons (HER) and one for positrons (LER). Each apparatus consists of three primary components: beamline, optical elements and detection system.

Beamline

Table 1: Beamline Parameters

Parameter	LER	HER	Unit
Energy	4	7	GeV
Source to optics (L)	9.259	10.261	m
Optics to detector (L′)	31.789	32.689	m
Air gap (f)	10	10	cm
Thickness of Be filter (T)	0.5	16	mm
Thickness of Be window (T′)	0.2	0.2	mm

* mulyani@post.kek.jp

Each of the SuperKEKB rings has four straight sections and four arc-bends. The X-ray sources are the last arc-bends located immediately upstream of the straight sections in Fuji (LER) and Oho (HER). The beamlines are about 40 m long from the source points to the detectors. A list of the parameters for the beamlines are shown in Table 1. The optical elements (pinhole and coded apertures) are located in optics boxes ≈9–10 m from the source points, for geometrical magnification factors of ≈3× for both lines. Beryllium filters are placed between source points and optic boxes to reduce the incident power levels for both lines. A 0.2 mm thick Be window is also placed at the end of each beamline to separate vacuum (beamline) and air (detector box).

Optical Elements

Three optical elements have been designed and installed in each ring: a single slit, a multi-slit coded aperture (17 slits) and a Uniformly Redundant Array (URA) coded aperture (12 slits) as shown in Fig. 1 [2]. These optical elements consist of 18–20 μm thick gold masking material on 600 μm thick diamond substrates.

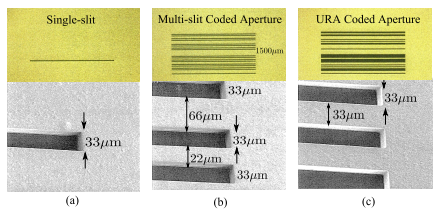

Figure 1: Three types of optical elements at 70× magnification and 1000× Scanning Electron Microscope (SEM): (a)Single-slit, (b) Multi-slit coded aperture and (c) URA coded aperture.

Detection System

For phase I of SuperKEKB commissioning, a cerium-doped yttrium-aluminum-garnet (YAG:Ce) scintillator is combined with a CCD camera for the x-ray imaging system as shown in Fig. 2. The resolution of this optical systems will be discussed in systematic resolution section.

GEOMETRICAL SCALE FACTORS

The geometrical scale factors based on beam-based measurement (see Fig. 3) are measured by moving either the beam or optical elements (single slit and coded apertures), observing how the peak features move, then calculating the ratio of geometric magnification M and scintillator camera

ISBN 978-3-95450-177-9

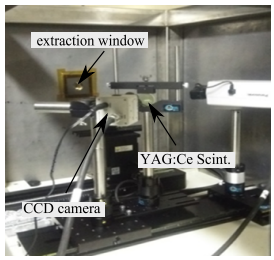

Figure 2: Detection system for phase I of SuperKEKB commissioning. Inside the detector box is a Be extraction window and a 141 μm thick YAG:Ce scintillator combined with CCD camera.

scale m (μm/pixel). When the beam is moved, the ratio M/m is determined by fitting Eq. 1:

$$P_1 = \Big(-\frac{M}{m}\big(1 - \frac{ds_1}{ds}\big)\Big) y_1 - \frac{M}{m}\frac{ds_1}{ds} y_2 + \alpha \qquad (1)$$

where P_1 is the position (in pixels) of a peak feature from x-rays that passed through a slit onto the scintillator, ds_1 is distance from source point to upstream BPM, ds is distance between upstream/downstream BPM and y_1, y_2 are y values (in μm) of the upstream and downstream BPMs, respectively. The parameter α represents the offset between beam and detector coordinate systems. When the mask is moved, the ratio $(M+1)/m$ is determined by fitting Eq. 2.

$$P_1 = \frac{M+1}{m} y_{mask} + \alpha \qquad (2)$$

where y_{mask} is the position of the mask in μm. Geometric magnification factors agree well between tape measurements and beam-based measurements at both lines, within 0.9–4.6 %, as shown in Table 2, where estimated systematic errors are shown for tape measurements, and statistical errors shown for beam-based measurements.

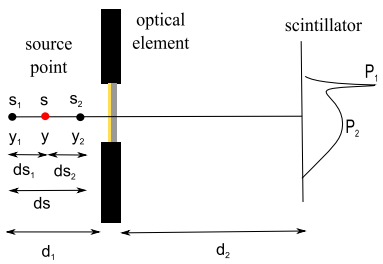

Figure 3: A schematic for the geometrical scale factors check, consisting of a source point with two BPMs at upstream and downstream, optical elements and peak feature images at scintillator detector. P_1 is the peak feature from an x-ray that passed through a slit onto the scintillator, and P_2 is the peak feature from x-rays that punched through the Au mask.

EMITTANCE CONTROL KNOB

The emittance control knob ratio method measures the overall scaling factor between the reported beam size measurements and the true beam size [3]. The variation of the vertical beam size by changing the bump height can be represented as:

$$(\sigma_y^{meas})^2 = (c\sigma_{y_0})^2 + (cA)^2(h - h_0)^2 \qquad (3)$$

with correlation between beam size σ_y, emittance ϵ_y and beta function β as:

$$\sigma_y = \sqrt{\epsilon_y \beta} \qquad (4)$$

where σ_{y_0} and σ_y^{meas} are the true vertical beam size and the beam size measured by the XRM. The parameters h and h_0 are the bump height and its offset, c is the calibration (scaling) factor and A is a linear coefficient where $A^2 = \Delta\epsilon_y \times \beta_y$, and $\Delta\epsilon_y$ is the expected change in emittance for a unit change in bump height. The values of $\Delta\epsilon_y$ and β_y given by the optics model are shown in Table. 3. The results of this method for both lines are shown in Figs. 4, 5 and Table 4, with a minimum beam size for the LER of 19 μm, and for the HER of 29 μm. By using Eq. 4 and the parameters in Table. 3, we can determine the vertical emittance for both rings: ϵ_y ≈11 pm (≈118 pm) for LER (HER). The value for the LER is close to the design value (≈ 10 pm), but is much higher than design for the HER. To investigate this discrepancy, a study of smearing factors (point spread functions) was made using beam lifetime data, in the next sub-section.

Table 2: Geometrical Scale Factors Check

Parameters		
LER (Tape Measurement)		
M/m	(pixels/mm)	66.2 ± 0.2(0.3 %)
(M+1)/m	(pixels/mm)	85.5 ± 0.2(0.2 %)
LER (Beam-Based Measurement)		
M/m	(pixels/mm)	69.5 ± 0.5(0.7 %)
(M+1)/m	(pixels/mm)	86.0 ± 0.6(0.65 %)
HER (Tape Measurement)		
M/m	(pixels/mm)	60.9 ± 0.2(0.3 %)
(M+1)/m	(pixels/mm)	80.0 ± 0.2(0.2 %)
HER (Beam-Based Measurement)		
M/m	(pixels/mm)	59.2 ± 0.5(0.9 %)
(M+1)/m	(pixels/mm)	79.3 ± 0.1(0.13 %)

Table 3: Beam Parameter

Parameter	LER	HER
$\Delta\epsilon_y$	70.0946 pm	43.0096 pm
β_y	67.1721 m	7.636 47 m

Lifetime Studies

The beam lifetime was also recorded during the emittance control knob studies. A bunch of charged particles (electrons/positrons) in a ring decay due to a variety of mechanisms: quantum lifetime (emission of synchrotron radiation), Coulomb scattering (elastic scattering on residual gas

ISBN 978-3-95450-177-9

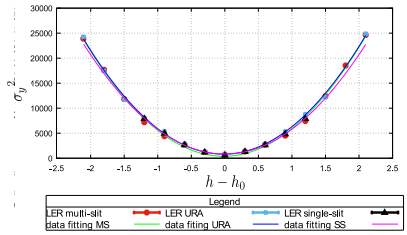

Figure 4: The LER emittance control knob data for all optical elements at 200 mA of beam current, with data points fitted by the function shown in Eq. 3.

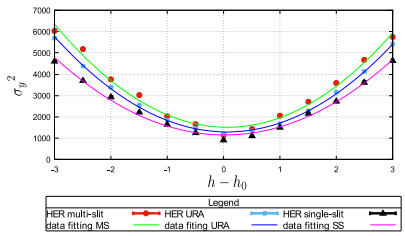

Figure 5: The HER emittance control knob data for all optical elements at 190–195 mA of beam current, with data points fitted by the function shown in Eq. 3.

atoms), Bremsstrahlung (photon emission induced by residual gas atoms) and the Touschek effect (electron-electron scattering). None of these mechanisms is related to the beam size except for the Touschek effect. The Touschek lifetime is related to the beam size as shown in Eq. 5 [4].

$$\frac{1}{\tau} = \frac{1}{\tau_{tk}} + \frac{1}{\tau_{qu}} + \frac{1}{\tau_{cs}} + \frac{1}{\tau_{bs}},$$
$$\frac{1}{\tau} = \frac{r_c^2 c Q}{8\pi e \sigma_y \sigma_x \sigma_z} \frac{\lambda^3}{\gamma^2} D(\epsilon) + C \qquad (5)$$

where τ is the total lifetime, τ_{tk} is the Touschek lifetime, $D(\epsilon)$ is the Touschek lifetime function (approximately constant for small ϵ), τ_{qu}, τ_{cs} and τ_{bs} are the quantum, coulomb and bremsstrahlung scattering lifetimes, respectively (written as a constant parameter C in Eq. 5). In this analysis, we only change the σ_y and the other parameters are constant, giving the simplified equation shown in Eq. 6.

Table 4: Emittance Control Knob Calibration

Mask	σ_{y0}(μm)	Cal. factor (c)
	LER	
single-slit	28.3 ± 1.1(3.9 %)	1.03 ± 0.01(1.0 %)
multi-slit	19.1 ± 4.3(22.4 %)	1.07 ± 0.01(0.9 %)
URA	27.4 ± 2.8(10.2 %)	1.06 ± 0.01(0.9 %)
	HER	
single-slit	30.9 ± 1.1 (3.6 %)	1.09 ± 0.02(1.8 %)
multi-slit	31.1 ± 1.5(4.9 %)	1.25 ± 0.03(2.4 %)
URA	29.9 ± 0.5(1.6 %)	1.20 ± 0.01(0.8 %)

$$\frac{1}{\tau} = \alpha \frac{1}{\sigma_y} + C \qquad (6)$$

By fitting $\frac{1}{\tau}$ vs $\frac{1}{\sigma_y}$ data via Eq. 6 (see Fig. 6), we obtained negative values for C, representing non-Touschek lifetime sources. The non-positive value of C indicates that the lifetime is heavily dominated by the Touschek lifetime, and further suggests the presence of a positive asymptote in the beam size.

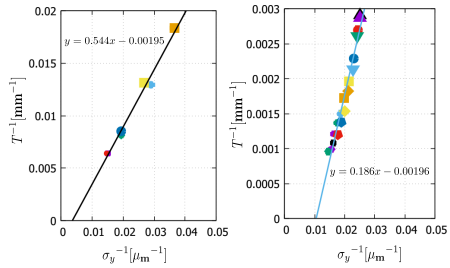

Figure 6: Relation between lifetime and beam size for multi-slit mask at LER (left) and HER (right) fitted by Eq. 6.

If a beam of initial size σ_{y_0} is convolved with a Gaussian smearing function of size σ_s to make a measured beam size σ_y^{meas}, then the measured beam size can be represented by adding the real beam size and the smearing size in quadrature as shown in Eq. 7.

$$\sigma_y^{meas} = \sqrt{(\sigma_{y_0})^2 + (\sigma_s)^2}$$
$$\sigma_{y_0} = \sqrt{(\sigma_y^{meas})^2 - (\sigma_s)^2} \qquad (7)$$

If we consider just the Toushek effect then the correlation between τ and σ_y^{meas} becomes:

$$\tau = \alpha \sigma_{y_0} = \alpha \sqrt{(\sigma_y^{meas})^2 - (\sigma_s)^2} \qquad (8)$$

Fitting the τ vs σ_y^{meas} data via Eq. 8 with α and σ_s as free parameters gives results like those shown (for multi-slit masks) in Fig. 7. By using Eq. 4 and the parameters in Table. 3, we can calculate the true minimum beam size σ_{y0} from the smallest measured beam size σ_y^{meas}, and corresponding vertical emittance ϵ_{y_0}. The average values over measurements made with all three optical elements, for σ_s, σ_{y0} and ϵ_{y_0} are shown in Table 5. From this table, we see that the smearing function for the HER is much larger than that for the LER. Also, even after accounting for this smearing function, the HER emittance is about 4 times larger than the design value.

SYSTEMATIC RESOLUTION

Based on the above discussion, there are smearing factors for both rings that need to be understood. Regarding the detector, there are some parameters that will affect the spatial resolution: defect of focus, diffraction effect and spherical

ISBN 978-3-95450-177-9

Table 5: The averages of smearing factor, minimum beam size and vertical emittance measured with all 3 optical elements

Parameter	LER	HER
σ_s	12.1 ± 2.1 μm	32.8 ± 0.4 μm
σ_{y_0}	23.5 ± 0.3 μm	17.8 ± 0.8 μm
ϵ_y	≈8 pm	≈41 pm

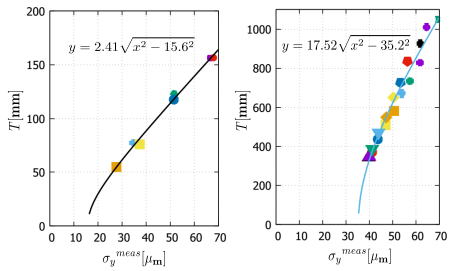

Figure 7: Relation between lifetime and beam size for multi-slit mask at LER (left) and HER (right) fitted by Eq. 8.

aberration [5]. If R_f is the spatial resolution, dz is the depth of the scintillator (141 μm), NA is the numerical aperture of the camera (0.03132), M is the magnification of the XRM (3.2) and λ is the wavelength of visible light from scintillator (550 nm), the relations between them are given as Eqs. 9-11.

$$R_f = \frac{dzNA}{M}, \text{defect of focus} \quad (9)$$

$$R_f = \frac{\lambda}{MNA}, \text{diffraction effect} \quad (10)$$

$$R_f = \frac{dz(NA)^2}{M}, \text{spherical aberration} \quad (11)$$

The effects contribute ≈ 5 μm of smearing as expressed at the source point. Besides those three effects, the resolution of detector can also be limited by the spatial distribution of the deposited energy imparted from ionizing radiation. This distribution is affected by scattered x-rays or secondary electrons that may deposit energy far away from the primary photon interaction site. EGS5 code[6] was used to calculate the absorbed dose of an x-ray pencil beam passing through the Be filter, optical elements, Be window and onto the flat surface of the 141 μm thick YAG scintillator, to determine the effect of scattering anywhere in the beam line or detector on the point spread function of the imaging system.

The geometry of the XRM beamlines used in the EGS5 simulation is shown in Fig. 8 and Table 1. The EGS5 calculation result seen in Fig. 9 shows that the scattered background falls off by an order of magnitude within 1 μm. Altogether, contributions from sources in Eqs. 9-11 and scattering effects (EGS5 simulation) only for sources of point spread in the XRM of ≈6 μm as expressed at the source point. This is insufficient to account for the observed smearing according to the lifetime studies. Other possible sources of smearing or resolution loss might be beam tilt or motion, camera misfocus or some source of scattering not simulated

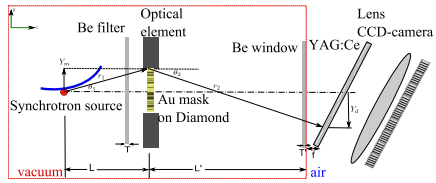

Figure 8: Schematic of XRM Beam Line. The beam passes through the Be filter, optical elements and Be window, and is then deposited in the 141 μm thick YAG scintillator.

by EGS5, such as impurities or inhomogeneities in the Be filters.

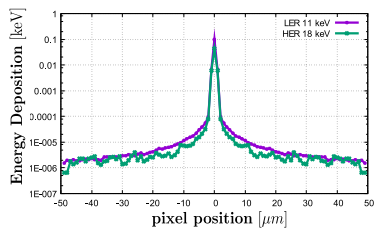

Figure 9: Deposited energy in YAG:Ce. The scattering range is <1 μm with a background/peak ratio of ≈ 10^{-4}.

CONCLUSION

We have presented some calibration studies during the Phase I of SuperKEKB commissioning. The geometrical magnification factors seem to be well understood for both LER and HER. The overall performance is reasonable for the LER, and yielded results consistent with expectations based on the optics estimation with ≈8 pm of vertical emittance (ϵ_y). For the HER, the vertical emittance ϵ_y is ≈41 pm which is 4× higher than the optics estimation. In addition, some smearing is observed, not all of which is fully accounted for yet. For our future plan, we plan to study possible sources of smearing either at the x-ray source point or in the beamline.

REFERENCES

[1] "SuperKEKB Design Report", https://kds.kek.jp/indico/event/15914/

[2] E.Mulyani, and J.W.Flanagan, *"Design of Coded Aperture Optical Elements for SuperKEKB X-ray Beam Size Monitors"*, in Proc. of IBIC2015, Melbourne, Sept 2015, TUPB025, pp. 377-380.

[3] N.Iida at al., *"Synchrotron Radiation Interferometer Calibration Check by Use of a Size Control Bump in KEKB"*, in Proc. of PAC07, Albuquerque, New Mexico, TUPAN042, pp. 1978-1480.

[4] H. Wiedemann, Particle Accelerator Physics I. Springer-Verlag Berlin Heidelberg, 2rd ed., 1999.

[5] A. Koch et al.,J. Opt. Soc. Am. A., Vol. 15, No. 7 pp. 1940-1951, July 1998.

[6] *The EGS5 Code System*, http://rcwww.kek.jp/research/egsegs5_manualslac730-130308.pdf

ISBN 978-3-95450-177-9